

Assessing sprinkler irrigation uniformity using a ballistic simulation model

by

Playán, E. ¹, Zapata, N. ², Faci, J. M. ², Tolosa, D.¹, Lacueva, J. L. ¹,

Pelegrín, J.² Salvador, R. ², Sánchez, I. ² and Lafita, A. ²

Abstract

Experiments were performed in the Ebro Valley of Spain to provide the basis for the calibration and validation of a ballistic simulation model of sprinkler irrigation. The experiments included evaluations of isolated sprinklers and solid-sets. Two different sprinklers, two principal nozzle diameters and three operating pressures were

¹ (✉) Dept. Genetics and Plant Production, Estación Experimental de Aula Dei (EEAD), CSIC, Apdo. 202, 50080 Zaragoza, Spain. Tel: +34 976 716 087. FAX: +34 976 716 145. Email: playan@eead.csic.es.

² Department of Soils and Irrigation, Centro de Investigación y Tecnología Agroalimentaria (CITA-DGA), Diputación General de Aragón. Apdo. 727, 50080 Zaragoza, Spain. Tel: +34 976 716 359. FAX: +34 976 716 335. Email: vzapata@aragon.es, jfaci@aragon.es

14 considered in the experiments, which also covered the usual range of wind speeds in
15 the study area. Model calibration served the objectives of predicting the Christiansen
16 Coefficient of Uniformity (*CU*) and the water application pattern. The resulting
17 standard error of *CU* estimation was 3.09 %. Tables of simulated uniformity were
18 produced for the two sprinklers using different nozzle diameters, sprinkler spacings,
19 operating pressures and wind speeds. These tables can be used for design and
20 management purposes, identifying options leading to adequate irrigation uniformity.
21 A simple simulation software has been produced and disseminated to assist irrigation
22 professionals and farmers in decision making.

23 **Introduction**

24 The uniformity of sprinkler irrigation depends on a number of factors, including the
25 sprinkler and nozzle type, the irrigation layout and the environment (Keller and
26 Bliesner, 1990). The combination of these factors greatly complicates the assessment of
27 irrigation uniformity for a given on-farm irrigation system and a set of environmental
28 conditions. As a consequence, sprinkler irrigation design and management rules are
29 very site specific, change with the irrigation materials, and often rely on unstructured
30 experiments and life-long professional experience.

31 Sprinkler irrigation has only limitedly benefited from modelling approaches. Ballistics
32 constitute the most common modelling approach to sprinkler irrigation. While the
33 theory behind this approach has been available for decades (Fukui et al., 1980), its
34 application is progressing quite slowly. The main problem for the generalization of
35 ballistic models is that model calibration is currently required for every combination of
36 sprinkler type, nozzle type and diameter, operating pressure, nozzle elevation and

37 wind speed (Montero et al., 2001). As a consequence, an intense experimental work is
38 required for the applicability of ballistic models for a particular situation. Once the
39 model is calibrated and validated, it can yield information leading to improved
40 irrigation design and management. Dechmi et al. (2004b) calibrated a ballistic model
41 for a particular irrigation layout under variable wind conditions. These authors
42 reported on a number of model applications for successful sprinkler irrigation in the
43 central Ebro Valley of Spain, a region where the yearly average of wind speed can
44 exceed 2.4 m s^{-1} .

45 In this paper we present the experimental and computational process required to
46 calibrate and validate a ballistic simulation model for two sprinklers, each with two
47 nozzle diameters, operating under a wide range of pressures and wind speeds, and
48 covering a large set of sprinkler spacings. The results permit to establish a comparison
49 between the two sprinklers, and to highlight their respective strengths and
50 weaknesses. Beyond the regional relevance of this comparison, the presented
51 methodology represents a contribution to the applicability of ballistic models to
52 sprinkler irrigation practice.

53 **Materials and Methods**

54 **Model description**

55 Fukui et al. (1980) presented the basic equations and procedures for ballistic simulation
56 of sprinkler irrigation. Their work was followed by a number of contributions which
57 improved the original approach in different aspects (Vories et al., 1987; Seginer et al.,
58 1991). Recently, Carrión et al. (2001) and Montero et al. (2001) presented the SIRIAS
59 software, which further developed ballistic theory and presented it in a user-friendly

60 environment. The SIRIAS model was calibrated and validated for a number of cases
61 involving different sprinklers and nozzle configurations, layouts and operating
62 conditions. The mean absolute error in the estimation of the Christiansen Coefficient of
63 Uniformity (*CU*) (Burt et al., 1997) was 2.7 %. Dechmi et al. (2004a; 2004b) presented a
64 ballistic sprinkler irrigation model which was used in combination with a crop model.
65 They showed that the sprinkler irrigation model could successfully reproduce the
66 water distribution pattern observed in the field ($R^2 = 0.871^{***}$). Moreover, a crop
67 simulation model using the simulated water distribution pattern as input resulted in
68 simulated values of yield reduction which could explain the field observed values ($R^2 =$
69 0.378^{***}).

70 The main characteristics of the ballistic model used in this work are presented in the
71 following paragraphs. Additional specifications can be found in Dechmi et al. (2004a),
72 who presented an early version of this model. General details the construction and
73 testing of ballistic models can be found in Carrión et al. (2001) and Fukui et al. (1980).

74 A sprinkler is simulated as a device emitting drops of different diameters. It is
75 assumed that drops are formed at the sprinkler nozzle, and travel independently until
76 reaching the soil surface (or the crop canopy, or the experimental catch can). In the
77 absence of wind, and for a given sprinkler configuration, the horizontal distance
78 between the drop landing point and the sprinkler nozzle is a function of the drop
79 diameter. Ballistic theory is used to determine the trajectory of each drop diameter
80 subjected to an initial velocity vector and a wind vector (\mathbf{U} , parallel to the ground
81 surface). The action of gravity (acting in the vertical direction) and the resistance force
82 (opposite to the drop trajectory) complete the analysis of forces acting on the water
83 drop. The drop velocity with respect to the ground (\mathbf{W}) is equal to the velocity of the
84 drop in the air (\mathbf{V}) plus the wind vector (\mathbf{U}).

85 According to Fukui et al. (1980) the three directional components of the movement of
 86 each drop can be expressed as:

$$87 \quad A_x = \frac{d^2x}{dt^2} = -\frac{3}{4} \frac{\rho_a}{\rho_x} \frac{C}{D} V(W_x - U_x) \quad [1]$$

$$88 \quad A_y = \frac{d^2y}{dt^2} = -\frac{3}{4} \frac{\rho_a}{\rho_W} \frac{C}{D} V(W_y - U_Y) \quad [2]$$

$$89 \quad A_z = \frac{d^2z}{dt^2} = -\frac{3}{4} \frac{\rho_a}{\rho_W} \frac{C}{D} V W_z - g \quad [3]$$

90 Where x , y , z are coordinates referring to the ground (with origin at the sprinkler
 91 nozzle), t is the time, ρ_a is the air density, ρ_W is the water density, A is the acceleration
 92 of the drop in the air, D is the drop diameter, and C is a drag coefficient, which can be
 93 expressed as a function of the Reynolds number of a spherical drop and the kinematic
 94 viscosity of the air (Fukui et al., 1980; Seginer et al., 1991):

95 Equations [1] to [3] are solved in the model using a fourth order Runge-Kutta
 96 numerical integration technique (Press et al., 1988). The main result of each drop
 97 trajectory solution is constituted by the x and y coordinates of the drop when the z
 98 coordinate equals 0 (the soil surface), or the crop canopy elevation, or the catch can
 99 elevation. In order to reproduce the water application pattern resulting from an
 100 isolated sprinkler, these equations must be solved for a number of horizontal sprinkler
 101 angles (due to the sprinkler rotation) and for a number of drop diameters. The model
 102 typically uses 180 horizontal sprinkler angles and 180 drop diameters, evenly
 103 distributed between 0.0002 and 0.007 m. When the landing coordinates of each drop
 104 diameter are combined with the fraction of the sprinkler discharge which is emitted in
 105 this drop diameter, the water application pattern can be simulated.

106 The measurement of sprinkler drop size has been performed using a variety of indirect
 107 methods. It is only recently that optical spectropuviometers have been used for
 108 sprinkler drop size characterization (Montero et al., 2003). These devices result in
 109 accurate and automated measurements. An alternative procedure consists on using the
 110 ballistic model to simulate the landing distance of different drop diameters resulting
 111 from a given sprinkler model, nozzle elevation and operating pressure in the absence
 112 of wind. The percentage of the irrigation water collected at each landing distance can
 113 be used to estimate the percentage of the irrigation water emitted in drops of a given
 114 diameter.

115 Li et al. (1994) proposed the following empirical model to fit the drop diameter
 116 distribution curve:

$$117 \quad P_v = \left(1 - e^{-0.693 \left(\frac{D}{D_{50}} \right)^n} \right) 100 \quad [4]$$

118 Where: P_v is the percent of total sprinkler discharge in drops smaller than D ; D_{50} is the
 119 mean drop diameter, and n is a dimensionless exponent. Equation [4] permits to
 120 establish a functional relationship between the drop diameter and the sprinkler
 121 discharge. The estimation of the parameters of this equation permits to characterize the
 122 drop diameter distribution resulting from a given sprinkler, nozzle diameter and
 123 operating pressure.

124 A significant part of the water emitted by a sprinkler does not reach the soil surface,
 125 because it either evaporates or drifts away. This water constitutes the Wind Drift and
 126 Evaporation Losses (*WDEL*), which are expressed as a percentage of the emitted
 127 discharge. Salvador (2003) and Playán et al. (2005) presented a number of empirical

128 equations aiming at the prediction of *WDEL* using meteorological variables. These
 129 authors used 37 solid-set experiments to formulate predictive equations. The following
 130 equation, obtained for daytime operation, was introduced in the model:

$$131 \quad WDEL = 24.1 + 1.41U - 0.216RH \quad [5]$$

132 where U is the wind speed (m s^{-1}) and RH is the relative humidity of the air (%).
 133 According to Montero et al. (2001) the magnitude of *WDEL* was used to adjust the drop
 134 size distribution curve. Option B, as presented by these authors, was used for this
 135 purpose.

136 Seginer et al. (1991) reported on the need to correct the drag coefficient in order to
 137 reproduce the deformation of the circular water application area produced by the
 138 wind. Tarjuelo et al. (1994) further refined these corrections, arriving to the following
 139 expression:

$$140 \quad C' = C(1 + K_1 \sin\beta - K_2 \cos\alpha) \quad [5]$$

141 Where: α is the angle formed by vectors V and U , β is the angle formed by the vectors V
 142 and W , and K_1 and K_2 are empirical parameters. According to Montero et al. (2001) K_2 is
 143 much less relevant than K_1 . This extreme was confirmed by the findings of Dechmi et
 144 al. (2004a). In order to maintain the generality of their model, Montero et al. (2001)
 145 recommended fixed values for K_1 and K_2 for different sprinkler materials and
 146 environmental conditions. To maximize the model predictive capability, Dechmi et al.
 147 (2004a) used wind-dependent values of both parameters for their particular
 148 experimental sprinkler set-up.

149 In order to simulate solid-set irrigation, the model overlaps a number of sprinklers
 150 located at coordinates reproducing a given sprinkler spacing. For this purpose, 16

151 sprinklers are used in rectangular layouts and 18 in triangular layouts. The central
152 sprinkler spacing is divided into a number of rectangular cells, with a default 5 x 5
153 arrangement. The resulting number of cells (25 in this case) must be equal to the
154 number of catch cans used in the field experiments.

155 Each drop landing in this central sprinkler spacing is assigned to one of the cells,
156 according to the landing co-ordinates. The simulated water application in each cell is
157 computed from the number of drops of each diameter and the percent of the sprinkler
158 discharge corresponding to that particular drop diameter. Water application in the
159 cells is further used to determine the simulated coefficient of uniformity. The process
160 of sprinkler overlapping is therefore performed following a mathematical rationale,
161 and is not subjected to any additional model parameter. This is why, once the model is
162 calibrated and validated, it can be used in sprinkler spacings different from the
163 experimental ones.

164 **Catch can size experiments**

165 A plastic commercial catch can (a rain gauge) with a diameter of 79 mm was found to
166 be well suited for the experiments, since it was marked in mm for direct readout (up to
167 40 mm), and it was mounted on a plastic stick for quick installation at 0.35 m over the
168 soil surface. The catch can was conical in its lower part (145 mm), and cylindrical in its
169 upper part (30 mm).

170 According to the relevant International Standards (Anonymous, 1987; Anonymous,
171 1990; Anonymous, 1995), the catch can diameter should exceed 85 mm. This criterion
172 was not met by the abovementioned catch can. The principle behind this diameter
173 requirement is that small catch cans can result in an underestimation of CU: the larger
174 the catch can, the higher the uniformity estimate. Taking the issue to a limit, if the catch

175 can size was equal to the sprinkler spacing, the *CU* estimate would always be 100%.
176 When uniformity is low (for instance, due to a high wind) this issue becomes
177 particularly important: small catch cans may artificially increase the existing
178 variability. While for practical purposes it is convenient to use small catch cans, this
179 choice should not compromise the quality of the uniformity estimations.

180 An experiment was devised to: 1) establish the effect of catch can size on *CU* and
181 *WDEL* under the windy, dry conditions of the Ebro valley of Spain; and 2) assess the
182 validity of the small catch can (79 mm in diameter). The experimental set-up and the
183 effect of catch can size on *WDEL* were reported by Playán et al. (2005). In this work, the
184 experimental set-up is summarily described, and the results for *CU* are presented and
185 discussed. The experiment involved the comparison of the small catch can (S) with two
186 larger, cylindrical catch cans with diameters of 130 and 210 mm (medium and large, M
187 and L, respectively).

188 The experiment was performed on a solid-set field with a R15x15 sprinkler spacing.
189 The sprinklers were VYR-70, and the nozzle diameters were 4.4 and 2.4 mm. The
190 nozzle height was 2 m, and the operating pressure was 380 kPa. 25 catch can locations
191 were evenly distributed within a central sprinkler spacing (5 rows by 5 columns, with a
192 3 m spacing). Three catch cans (S, M and L) were installed at each location, separated
193 0.3 m in a triangular arrangement. The location of each catch can at the vertices of this
194 triangle was randomised. The upper part of all catch cans was located 0.50 m over the
195 soils surface. A total of thirteen 3-hour irrigation experiments were performed. The
196 operating pressure, the meteorological conditions and the catch can readings (3 x 25)
197 were recorded in every experiment. The *CU* was determined in each experiment for
198 each type of catch can.

199 The statistical analysis was based on the relationship between the differences in CU
200 estimated with the different catch cans and the wind speed. At low wind speeds CU
201 was very high (typically about 95 %), and the differences in CU among the three catch
202 cans were non-relevant. If a regression line can be statistically established between the
203 wind speed and the differences in CU estimation between two types of catch cans, then
204 both catch cans perform differently, with the large one being potentially more accurate
205 under windy conditions

206 **Water application experiments**

207 Field experiments were designed taking into consideration the recommendations of
208 Merriam and Keller (1978), and the relevant international standards (Anonymous,
209 1987; Anonymous, 1990; Anonymous, 1995).

210 Two different sprinklers, frequently installed in the Ebro Valley of Spain, were used in
211 this research: the RC-130H from Riegos Costa (Lleida, Spain) and the VYR-70 from
212 VYRSA (Briviesca, Burgos, Spain) (the citation of commercial trademarks does not
213 imply endorsement). Both sprinklers were analysed with their principal nozzles of 4.0
214 and 4.4 mm, and an auxiliary nozzle of 2.4 mm. The principal nozzles were equipped
215 with the straightening vanes provided by the manufacturer. The nozzle elevation was
216 2.0 m above the soil surface. This nozzle elevation is widely used in the study area
217 since corn is a very common crop.

218 Each combination of sprinkler and principal nozzle diameter was tested at three nozzle
219 operating pressures: 200, 300 and 400 kPa. The experimental tests were performed in
220 isolated sprinklers and in a rectangular 18 x 15 m (R18x15) solid-set arrangement. The
221 gross application rate ranged from 4.4 to 7.2 mm h⁻¹.

222 In the isolated sprinkler experiments precipitation was recorded along four radii, at
223 distances from the sprinkler ranging from 0.5 to 15.5 m, with an increment of 0.5 m.
224 The results of the four radii were averaged to produce the radial water application
225 pattern. All the experiments performed with isolated sprinklers lasted for 2 hours and
226 were performed under low wind conditions. A total of 12 isolated sprinkler
227 experiments were performed (2 sprinklers \times 2 principal nozzle diameters \times 3 operating
228 pressures).

229 A rectangular 4 \times 4 sprinkler set-up was used for the solid set, with the experimental
230 area located between the four central sprinklers. A matrix of 5 \times 5 catch cans was
231 installed at a spacing of 3.6 \times 3.0 m, covering the experimental sprinkler spacing. Each
232 solid-set experiment was repeated under different wind speed conditions, in an
233 attempt to characterize the water distribution pattern resulting from different
234 combinations of sprinkler, principal nozzle diameter, operating pressure and wind
235 speed. All solid-set experiments lasted for 3 hours. Table 1 presents the average wind
236 speed and the *CU* resulting from all solid-set experiments. Of the 43 solid-set
237 experiments, 36 were used for model calibration and 7 for model validation. The
238 number of experiments performed for each combination of sprinkler, principal nozzle
239 diameter and operating pressure varied from 3 to 5. This variability resulted from the
240 difficulties in obtaining uniform wind speed and direction during the whole
241 experiment, from the replications needed to obtain adequate coverage of the usual
242 wind speed range, and from the need for validation experiments in the same
243 conditions. Tolosa (2003) presented further details on this set of field experiments.

244 Additional experiments were performed to further validate the model in other
245 sprinkler spacings. 50 experiments were performed with sprinklers RC-130H and
246 4.4+2.4 mm nozzles using triangular spacings of 18 \times 18 m (T18x18) and 18 \times 15 m

247 (T18x15). 37 experiments were performed on a R15x15 solid set equipped with VYR-70
248 sprinklers and 4.4+2.4 mm nozzles.

249 An automated weather station located in the experimental field recorded air
250 temperature, relative humidity and wind speed and direction at 5 min intervals.

251 **Model calibration**

252 The first step of the validation process consisted on determining the parameters D_{50}
253 and n that result in best agreement between the model results and the experimental
254 radial water application pattern obtained from isolated sprinklers in the absence of
255 wind. The following procedure was repeated for each sprinkler, nozzle diameter and
256 operating pressure.

257 A range of D_{50} and n pairs of values were explored (D_{50} from 0.0014 to 0.0023 m, with
258 an increment of 0.0001 m; n from 1.9 to 2.8, with an increment of 0.1). The resulting 100
259 simulations were sorted in decreasing order of the ratio $r/RMSE$, where r is the
260 correlation coefficient between observed and simulated radial precipitation, and $RMSE$
261 is the root mean square error. High values of this ratio ensure a high correlation and a
262 low estimation error.

263 The next step was to simulate the experimental solid set at zero wind speed using
264 different combinations of D_{50} and n , and starting from the top of the list. Typically, the
265 upper parameter values in the list resulted in lower CU than the closest experimental
266 values (the lowest wind experiments). A sensitivity analysis showed that the simulated
267 CU very much depended on the value of n . As a consequence, the irrigation event was
268 simulated with the optimum D_{50} and lower than optimum values of n . The procedure
269 was repeated till a pair of parameters was found that resulted in an adequate CU

270 estimation, while still reproducing the radial water application pattern in a satisfactory
271 way (with adequate values of r and $RMSE$).

272 The next step was the calibration of K_1 and K_2 . For each of the 36 solid-set experiments
273 devoted to model calibration, simulations were performed using values of K_1 from 0.0
274 to 2.8 (with increments of 0.2), and values of K_2 from 0.0 to 0.95 (with increments of
275 0.05). Each of the 266 resulting simulations was confronted with the experimental
276 results of catch can irrigation depth and CU . Out of this comparison, three indexes
277 were determined: r , $RMSE$ and the absolute difference between observed and
278 simulated CU (CU_d). The simulation results were again sorted by decreasing values of
279 $r/RMSE$, and pairs of K_1 and K_2 values were selected that ranked in the upper 10 % of
280 the list and had values of CU_d typically lower than $\pm 1\%$. This procedure ensures that
281 the model will produce an adequate prediction of CU , and at the same time, the spatial
282 distribution of irrigation water within the sprinkler spacing will be reproduced.
283 Obtaining both goals simultaneously leads to sacrificing some accuracy in each of
284 them. On the positive side, the resulting model will be fit for irrigation engineering and
285 agronomic applications (Dechmi et al., 2004b).

286 The resulting values of D_{50} , n , K_1 and K_2 were built into the calibrated model, and linear
287 interpolation among the parameters was introduced to simulate values of operating
288 pressure and wind speed not considered in the calibration phase.

289 **Model validation**

290 The first step of model validation consisted on simulating the seven irrigation events
291 which were not used for calibration purposes, and comparing the model simulated and
292 experimental values of CU .

293 In a second step, the 87 additional solid-set validation experiments were used. The
294 experimental conditions were introduced in the model. Simulated and experimental
295 values of *CU* were compared for the three different sprinkler spacings. This validation
296 experiment served to evaluate the capacity of the model to reproduce irrigation events
297 in solid-set spacings and operating pressures different from the ones used for
298 calibration.

299 **Model application**

300 The validated model was used to estimate *CU* in different conditions. The simulations
301 included the two sprinklers, the two nozzle diameters, five operating pressures (200,
302 250, 300, 350 and 400 kPa), 9 wind speeds (from 0 to 8 m s⁻¹, with an increment of
303 1 m s⁻¹), two types of sprinkler spacings (triangular and rectangular), and four
304 sprinkler spacings (15x12, 18x15, 18x18 and 21x18). The results of these 1,440
305 simulations were organized in a tabular form in order to provide for a comparison of
306 the relative performance of each sprinkler under different irrigation set-ups,
307 operational and environmental conditions.

308 **Results and discussion**

309 **Effects of catch can size on irrigation uniformity**

310 Differences in *CU* between the three considered catch cans were found to be minimal
311 when the wind speed was between 0 and 2 m s⁻¹, as presented in Figure 1. Statistical
312 relationships between wind speed and the differences in *CU* could be established
313 between the large catch can (210 mm in diameter) and the other two. The resulting
314 regression equations and the coefficients of determination are presented in Figure 1.

315 No statistical differences were found between the small catch can (S, 79 mm in
316 diameter), and the medium catch can (M, 130 mm in diameter), which is way larger
317 than required by the International Standard (minimum diameter of 85 mm). It could
318 therefore be concluded that using the experimental catch can (S) does not result in
319 significant errors in *CU* estimation respect to the minimum diameter requirement.

320 However, the comparison with the large catch can does cast some doubts, since at large
321 wind speeds (6-8 m s⁻¹) the small and medium catch cans resulted in lower estimates of
322 *CU*. It is reasonable to assume that the large catch can produces better estimates of *CU*
323 than the other two. However, the issue of catch can size (and shape) will require
324 additional research.

325 With these precautions in mind, the small catch can was retained for use in all the
326 experiments described in this paper. The regression equation L-S could be used to
327 estimate the *CU* corresponding to the large catch can from the *CU* obtained with the
328 small catch can.

329 **Calibration of d_{50} and n**

330 The results of the calibration procedure are presented in Table 2. Dechmi et al. (2004a)
331 analysed one of the cases presented in this table: sprinkler VYR-70 with 4.4 + 2.4 mm
332 nozzles at an operating pressure of 300 kPa. For this particular case, our results show
333 that the parameter combination ranking highest in terms of $r/$ RMSE is $D_{50} = 0.0017$ m
334 and $n = 2.45$ ($r = 0.83$; $RMSE = 1.08$ mm h⁻¹). Dechmi et al. (2004a) found an optimum
335 combination of $D_{50} = 0.0013$ m and $n = 2.50$ ($r = 0.79$; $RMSE = 0.48$ mm h⁻¹). For a
336 generic medium-sized impact sprinkler, Kincaid et al. (1996) measured drop size
337 distribution an arrived to $D_{50} = 0.0021$ m and $n = 1.82$. The differences between our
338 results and those of Dechmi et al. (2004a) are not particularly relevant in practical

339 terms. For instance, the comparison of the simulation results using the optimum
340 parameters found by Dechmi et al. (2004a) with the experiments reported in this paper
341 would result in $r = 0.87$ and $RMSE = 2.35 \text{ mm h}^{-1}$; a very good correlation and a
342 somewhat large error. The optimum experimental results still need to be adjusted to
343 perform in terms of uniformity estimation. The CU obtained at the lowest wind speed
344 ($U = 1.4 \text{ m s}^{-1}$) was 93.6 % (Table 1). Simulations performed at zero wind speed should
345 therefore result in a uniformity higher than 93.6 %. This was first obtained for $D_{50} =$
346 0.0017 m and $n = 1.90$ ($CU = 95.0\%$). As a consequence, this set of parameters was
347 retained.

348 The values of D_{50} decrease with the operating pressure and, in the case of the RC-130H,
349 with the nozzle diameter (Table 2). For sprinkler VYR-70 operating at a pressure of
350 400 kPa , D_{50} decreases as the nozzle diameter increases. This may be explained by the
351 fact that, as previously discussed, different parameter combinations result in adequate
352 simulation of the water application pattern. The values of $RMSE$ ranged from 1.09 to
353 3.64 mm h^{-1} . The coefficient of correlation remained in the range of 0.50 to 0.83.

354 **Calibration of K_1 and K_2**

355 Table 1 presents the optimum values of K_1 and K_2 for each of the calibration
356 experiments, together with the resulting values of $RMSE$ and r . The correlation
357 coefficients ranged from 0.18 to 0.84, with an average of 0.65. The lowest correlation
358 coefficients correspond to high uniformities ($CU > 85\%$). In these irrigation events the
359 variability in irrigation depth is small and the experimental error may account for a
360 large part of the variability. The $RMSE$ ranged from 0.41 to 2.11 mm h^{-1} , with an
361 average of 0.96 mm h^{-1} . These figures of $RMSE$ amount to between 3 and 19 % of the

362 gross irrigation depth applied by each combination of nozzle diameter and operating
363 pressure in the experimental R18x15 sprinkler spacing.

364 The goal of the calibration was to maintain low values of *RMSE* and high values of *r*,
365 while producing accurate predictions of *CU*. Figure 2a presents a plot of experimental
366 *vs.* calibration values of *CU*. A regression line was established with $R^2 = 0.977^{***}$. The
367 regression slope and the intercept were not significantly different from 1 and 0,
368 respectively, at the 95 % probability level. Uniformity was accurately predicted, with a
369 standard error of the linear regression model of 1.48 %.

370 **Model validation**

371 In a first step, the model was validated with data from the same series of experiments
372 as the calibration data set. Figure 2b shows a scatter plot of experimental *vs.* simulated
373 *CU* for the seven validation experiments. A regression analysis proved significant
374 ($R^2 = 0.855^{**}$), and revealed that the regression slope and the intercept were not
375 significantly different from 1 and 0, respectively (95 % probability level). The standard
376 error of *CU* estimation was 3.09 % .

377 Figure 3 presents the results of the second validation step. Experimental values of *CU*
378 were plotted against wind speed for the three different sprinkler spacings. A series of
379 simulated data corresponding to the experimental conditions and wind speeds at
380 increments of 1 m s^{-1} was added to the three subplots. The simulated data reproduced
381 the basic features of the experimental data set, although the variability was larger than
382 in the first step. The simulation model showed predictive capacity at sprinkler spacings
383 and operating pressures different from the experimental ones.

384 **Development of uniformity tables and a simulation software**

385 Tables 3, 4, 5 and 6 present the results of simulated *CU* for the two sprinkler types, two
386 nozzle diameters, eight sprinkler spacings and nine wind speeds (0 - 8 m s⁻¹). The tables
387 were produced for management and design purposes.

388 At the management level, farmers must take quick irrigation decisions for a given
389 sprinkler layout, operating pressure and wind speed. The latter two variables are often
390 related in collective irrigation networks, since high wind spells reduce water demand,
391 and may lead to an increase the operating pressure. As soon as the windy period is
392 over, most farmers decide to turn their systems on, and the operating pressure can
393 drop substantially due to a high simultaneity. The proposed tables can be used for *a*
394 *priori* estimation of the *CU* resulting from irrigating under a particular pressure and
395 wind speed.

396 In an experiment on sprinkler irrigated corn, Dechmi et al. (2003) found that the
397 irrigation water applied when the wind speed was higher than 2.1 m s⁻¹ (*CU* lower than
398 84 %) was significantly correlated with corn yield. Farmers could adopt *CU*
399 management thresholds depending on the crop value and the on-farm irrigation
400 equipment. An adequate selection of the proper irrigation timing (avoiding high
401 winds) would lead to increased water conservation (reducing deep percolation losses
402 and wind drift and evaporation losses) and increased crop yield (Dechmi et al., 2004b;
403 Playán et al., 2005).

404 Additionally, these tables could be used as the basis of irrigation programmers capable
405 of making advanced irrigation decisions. The user would preset a given irrigation
406 depth, and the programmer would select the most appropriate irrigation timing to
407 attain maximum *CU* and minimize *WDEL*. In order to make the right decisions the

408 programmer should have access to variables such as wind speed, relative humidity (for
409 *WDEL* estimation), and pressure at the hydrant.

410 At the irrigation system design phase, tabulated simulation results can be used to
411 determine the adequate sprinkler model, nozzle diameter, operating pressure and
412 spacing that can yield adequate performance under the wind pattern of a certain
413 location. Table 7 has been prepared to illustrate such process. The Table presents the
414 sprinkler producing higher uniformity under each parameter combination. When the
415 absolute value of the difference in *CU* is smaller than or equal to the standard error of
416 *CU* estimation in the validation (3.09 %), we can not conclude that one sprinkler
417 performs better than the other. These cases are labelled as “indifference” in Table 7.

418 In general, the comparison between both sprinklers does not depend on the type of
419 sprinkler spacing (rectangular *vs.* triangular). While for a principal nozzle diameter of
420 4.0 mm the RC-130H shows better performance than the VYR-70, for the 4.4 mm nozzle
421 the situation is more balanced. At narrow sprinkler spacings RC-130H performs better
422 than VYR-70, while at ample spacings the situation is somewhat reversed. For wind
423 speeds in the range of 2 to 5 m s⁻¹, RC-130H performed better than VYR-70. The relative
424 performance of both sprinklers at low or extreme winds very much depends on the
425 particular case.

426 A simulation software (only available in Spanish) has been produced to further
427 disseminate the results of this research. The software has been designed for irrigation
428 professionals and advanced farmers. Simulation parameters have been implemented
429 internally, and the user interaction has been limited to the common technical variables.
430 Software output includes a water application map within the solid-set spacing,
431 summary statistics on water application and wind drift and evaporation losses, and an

432 irrigation recommendation. Research in underway to increase the choice of available
433 sprinklers in the software. The simulation software can be freely downloaded from
434 [www.?](#).

435 Conclusions

436 The proposed methodology for the calibration and validation of the ballistic model has
437 permitted to generate 1,440 discrete estimations of irrigation uniformity (involving a
438 number of different solid set spacings) from just 12 isolated sprinkler evaluations and
439 43 solid set evaluations. The resulting model has proven to have a satisfactory
440 predictive capacity (the calibration standard error for *CU* was 3.09 %), and permits to
441 reduce the experimental work by 96 %. However, the required experimental effort is
442 still important, and must be performed under strict quality control, since the model
443 calibration procedure will amplify any experimental error.

444 Model simulation output tables have permitted to identify the conditions best suited
445 for each sprinkler. As a consequence, technical criteria can be used for the selection of
446 the adequate sprinkler and nozzle diameter for the prevailing operation and
447 environmental conditions at a given location. *CU* tables can also be used in a given
448 sprinkler layout to optimise irrigation management in response to the operating
449 pressure and the wind speed. These tables could be implemented in advanced
450 irrigation programmers, whose primary objective would be to guarantee a minimum
451 irrigation uniformity in all irrigation events. In order to ensure the applicability of the
452 model in an irrigated area, it will be important to estimate the calibration parameters
453 for the most relevant sprinklers and nozzle diameters. Consequently, the required
454 experimental effort may limit the benefits of the proposed methodology. On the other

455 hand, in a context of growing concerns about water availability, it is very important
456 that this information is made available to farmers and irrigation specialists.

457 **Acknowledgement**

458 This research was funded by the CONSI+D of the Government of Aragón (Spain)
459 through grant P028/2000 and by the Plan Nacional de I+D+I of the Government of
460 Spain through grant AGL2004-06675-C03/AGR. Thanks are also due to Miguel
461 Izquierdo, Jesús Gaudó and Enrique Mayoral for their support in the field.

462 **References**

- 463 Anonymous, 1987. Procedure for sprinkler distribution testing for research purposes.
464 ASAE, St. Joseph, MI, USA. pp. 487-489.
- 465 Anonymous, 1990. Agricultural irrigation equipment. Rotating sprinklers. Part 2.
466 Uniformity of distribution and test methods. ISO standard 7749/2. ISO. Geneva,
467 Switzerland.
- 468 Anonymous, 1995. Agricultural irrigation equipment. Rotating sprinklers. Part 1.
469 Design and operational requirements. ISO standard 7749/1. ISO. Geneva,
470 Switzerland.
- 471 Burt, C. M., Clemmens, A. J., Strelkoff, T. S., Solomon, K. H., Bliesner, R. D., A., H. L.,
472 Howell, T. A. and Eisenhauer, D. E., 1997. Irrigation performance measures:
473 efficiency and uniformity. *J. Irrig. Drain. Div., ASCE*, 123(6):423-442.
- 474 Carrión, P., Tarjuelo, J. M. and Montero, J., 2001. SIRIAS: a simulation model for
475 sprinkler irrigation: I. Description of the model. *Irrig. Sci.*, 2001(20):73-84.
- 476 Dechmi, F., Playán, E., Cavero, J., Faci, J. M. and Martínez-Cob, A., 2003. Wind effects
477 on solid set sprinkler irrigation depth and corn yield. *Irrig. Sci.*, 22, 67-77.
- 478 Dechmi, F., Playán, E., Cavero, J., Martínez-Cob, A. and Faci, J. M., 2004a. A coupled
479 crop and solid set sprinkler simulation model: I. Model development. *J. Irrig. and*
480 *Drain. Engrg., ASCE*, 130(6):499-510.

- 481 Dechmi, F., Playán, E., Cavero, J., Martínez-Cob, A. and Faci, J. M., 2004b. A coupled
482 crop and solid set sprinkler simulation model: II. Model application. *J. Irrig. and*
483 *Drain. Engrg., ASCE*, 130(6):511-519.
- 484 Fukui, Y., Nakanishi, K. and Okamura, S., 1980. Computer evaluation of sprinkler
485 irrigation uniformity. *Irrig. Sci.*, 2:23-32.
- 486 Keller, J. and Bliesner, R. D., 1990. *Sprinkle and trickle irrigation*. Van Nostrand
487 Reinhold, New York, NY. 652 pp.
- 488 Kincaid, D. C., Solomon, K. H. and Oliphant, J. C., 1996. Drop size distributions for
489 irrigation sprinklers. *Trans. ASAE*, 39(3):839-845.
- 490 Li, J., Kawano, H. and Yu, K., 1994. Droplet size distributions from different shaped
491 sprinkler nozzles. *Trans. ASAE*, 37(6):1871-1878.
- 492 Merriam, J. L. and Keller, J., 1978. *Farm irrigation system evaluation: a guide for*
493 *management*. Utah State University, Logan, Utah. 271 pp.
- 494 Montero, J., Tarjuelo, J. M. and Carrión, P., 2001. SIRIAS: a simulation model for
495 sprinkler irrigation: II. Calibration and validation of the model. *Irrig. Sci.*,
496 2001(20):85-98.
- 497 Montero, J., Tarjuelo, J. M. and Carrión, P., 2003. Sprinkler droplet size distribution
498 measured with an optical spectrop pluviometer. *Irrig. Sci.*, 2003(22):47-56.
- 499 Playán, E., Salvador, R., Faci, J. M., Zapata, N., Martínez-Cob, A. and Sánchez, I., 2005.
500 Day and night wind drift and evaporation losses in sprinkler solid-sets and moving
501 laterals. *Agric. Wat. Manage.*, In press.

- 502 Press, W. H., Flannery, B. P., Teukolsky, S. A. and Vetterling, W. T., 1988. Numerical
503 recipes in C. Cambridge University Press, Cambridge. 735 pp.
- 504 Salvador, R., 2003. Estudio de las pérdidas por evaporación y arrastre en los sistemas
505 de riego por aspersión. Diferencias entre riegos diurnos y nocturnos. Unpublished
506 graduation report. Universitat de Lleida. Lleida, Spain. 179 pp.
- 507 Seginer, I., Nir, D. and von Bernuth, D., 1991. Simulation of wind-distorted sprinkler
508 patterns. *J. Irrig. and Drain. Engrg., ASCE*, 117(2):285-306.
- 509 Tarjuelo, J. M., Carrión, P. and Valiente, M., 1994. Simulación de la distribución del
510 riego por aspersión en condiciones de viento. *Inv. Agr.: Prod Prot. Veg.*, 9(2):255-
511 271.
- 512 Tolosa, D., 2003. Calibración de un modelo balístico de riego por aspersión para
513 diferentes diámetros de boquilla, presiones e intensidades de viento. Unpublished
514 graduation report, Universitat de Lleida, Lleida, Spain. 105 pp.
- 515 Vories, E. D., D., v. B. R. and Mickelson, R. H., 1987. Simulating sprinkler performance
516 in wind. *J. Irrig. Drain. Div., ASCE*, 113(1):119-130.
- 517

518 **List of Tables**

519 **Table 1.** *Characteristics of the field experiments for the RC-130H and VYR-70 sprinklers. Each*
520 *experiment is characterized by the nozzle diameter (D , mm), the operating pressure (P , kPa),*
521 *the wind speed (U , $m\ s^{-1}$) and the Coefficient of Uniformity (CU, %). The use of each*
522 *experiment for either calibration (C) or validation (V) purposes is also reported in the table.*
523 *The calibrated values of parameters $K1$ and $K2$, and the agreement indexes Root Mean Square*
524 *Error (RMSE) and coefficient of correlation (r) are also presented.*

525 **Table 2.** *Selection of model parameters D_{50} and n for each isolated sprinkler experiment. The*
526 *root mean square error (RMSE) and coefficient of correlation (r) between observed and*
527 *simulated data are presented for each case.*

528 **Table 3.** *CU (%) resulting from different triangular sprinkler spacings, nozzle pressures and*
529 *wind speeds for the RC-130H and VYR-70 sprinklers, using 4.0 and 2.4 mm nozzles.*

530 **Table 4.** *CU (%) resulting from different triangular sprinkler spacings, nozzle pressures and*
531 *wind speeds for the RC-130H and VYR-70 sprinklers, using 4.4 and 2.4 mm nozzles.*

532 **Table 5.** *CU (%) resulting from different rectangular sprinkler spacings, nozzle pressures and*
533 *wind speeds for the RC-130H and VYR-70 sprinklers, using 4.0 and 2.4 mm nozzles.*

534 **Table 6.** *CU (%) resulting from different rectangular sprinkler spacings, nozzle pressures and*
535 *wind speeds for the RC-130H and VYR-70 sprinklers, using 4.4 and 2.4 mm nozzles.*

536 **Table 7.** *Sprinkler resulting in higher CU (%) for each combination of spacing, main nozzle*
537 *diameter (mm), operating pressure (kPa) and Wind Speed ($m\ s^{-1}$).*

538 **Table 1.** Characteristics of the field experiments for the RC-130H and VYR-70 sprinklers. Each
 539 experiment is characterized by the nozzle diameter (D , mm), the operating pressure (P , kPa),
 540 the wind speed (U , $m\ s^{-1}$) and the Coefficient of Uniformity (CU , %). The use of each
 541 experiment for either calibration (C) or validation (V) purposes is also reported in the table.
 542 The calibrated values of parameters K_1 and K_2 , and the agreement indexes Root Mean Square
 543 Error (RMSE) and coefficient of correlation (r) are also presented.

544

D (mm)	P (kPa)	RC-130H						VYR-70							
		U (ms^{-1})	CU (%)	K1	K2	RMSE ($mm\ h^{-1}$)	r	Use -	U (ms^{-1})	CU (%)	K1	K2	RMSE ($mm\ h^{-1}$)	r	Use -
4.0	200	0.9	85.7	0.0	0.00	0.61	0.63	C	2.0	85.8	1.0	0.35	0.84	0.33	C
		3.8	81.7	1.2	0.25	0.57	0.84	C	2.5	82.9	-	-	-	-	V
		5.4	71.3	1.6	0.40	0.90	0.83	C	3.4	73.2	1.8	0.60	0.85	0.72	C
	300	1.2	91.8	-	-	-	-	V	6.9	69.1	1.2	0.65	0.95	0.72	C
		1.8	84.9	2.2	0.20	0.75	0.62	C	1.8	87.6	1.6	0.20	0.63	0.67	C
		2.8	86.6	-	-	-	-	V	2.9	73.1	2.4	0.50	1.08	0.73	C
		3.0	84.9	1.6	0.25	0.67	0.73	C	8.4	68.3	1.0	0.55	1.38	0.60	C
		3.2	83.4	1.6	0.15	0.69	0.70	C							
		1.7	91.1	0.0	0.00	0.75	0.33	C							
	400	2.0	88.0	-	-	-	-	V	0.4	92.9	0.2	0.05	0.72	0.29	C
		2.4	91.0	1.2	0.10	2.06	0.61	C	4.2	74.8	2.4	0.50	0.93	0.83	C
		3.9	78.4	1.4	0.20	0.83	0.81	C	9.3	60.3	2.6	1.00	1.29	0.80	C
4.4	200	1.3	86.5	0.6	0.00	0.69	0.55	C	1.2	87.6	-	-	-	-	V
		2.1	91.0	1.0	0.10	0.41	0.73	C	1.7	89.4	0.6	0.25	0.83	0.46	C
		7.6	71.6	1.8	0.15	1.20	0.84	C	4.0	74.4	0.8	0.65	0.97	0.73	C
	300	1.1	90.2	0.4	0.00	0.56	0.73	C	7.9	71.0	1.0	0.60	1.11	0.68	C
		1.5	92.3	-	-	-	-	V	1.4	93.6	0.4	0.10	0.51	0.29	C
		3.6	83.8	1.4	0.15	0.69	0.80	C	2.2	88.9	0.8	0.30	0.57	0.72	C
		7.6	69.4	1.8	0.45	1.73	0.72	C	6.8	71.0	1.0	0.55	1.13	0.66	C
	400	1.1	91.2	0.0	0.00	0.81	0.41	C							
		4.3	75.7	2.4	0.05	1.28	0.74	C	0.7	93.9	0.2	0.10	0.66	0.18	C
		7.2	68.9	2.4	0.25	2.11	0.63	C	4.0	80.8	1.8	0.40	0.84	0.83	C
									5.2	70.4	-	-	-	-	V
								7.0	62.6	2.8	0.95	1.87	0.81	C	

545

546

547 **Table 2.** Selection of model parameters D_{50} and n for each isolated sprinkler experiment. The
 548 root mean square error (RMSE) and coefficient of correlation (r) between observed and
 549 simulated data are presented for each case.

550

551

Sprinkler	Nozzle Diameter (mm)	Nozzle Pressure (kPa)	D_{50} (m)	n (-)	RMSE (mm h ⁻¹)	r (-)
RC-130H	4.0	200	0.0019	2.0	1.23	0.80
		300	0.0017	2.0	1.82	0.70
		400	0.0015	2.2	3.64	0.50
	4.4	200	0.0021	1.9	1.71	0.66
		300	0.0017	2.1	1.92	0.68
		400	0.0017	2.0	2.12	0.63
VYR-70	4.0	200	0.0019	2.0	1.16	0.81
		300	0.0017	2.2	1.09	0.83
		400	0.0017	2.0	1.67	0.77
	4.4	200	0.0019	1.9	1.83	0.73
		300	0.0017	1.9	2.64	0.66
		400	0.0016	2.0	2.23	0.73

552

553 **Table 3.** *CU (%) resulting from different triangular sprinkler spacings, nozzle pressures and*
 554 *wind speeds for the RC-130H and VYR-70 sprinklers, using 4.0 and 2.4 mm nozzles.*

555

556

	P (kPa)	RC-130H										VYR-70							
		U (m s ⁻¹)										U (m s ⁻¹)							
		0	1	2	3	4	5	6	7	8	0	1	2	3	4	5	6	7	8
T 15 x 12	200	90	89	88	88	86	84	84	83	83	90	89	87	83	82	79	77	77	74
	250	94	93	91	90	88	86	85	83	81	91	90	89	85	82	80	77	76	72
	300	96	95	93	91	90	86	87	84	81	91	91	90	86	82	79	78	74	72
	350	95	94	92	90	89	86	85	83	80	96	95	93	89	85	81	78	75	75
	400	93	92	90	89	86	86	83	82	79	99	98	95	92	87	83	77	77	75
T 18 x 15	200	81	81	84	90	90	82	76	72	68	81	82	83	80	77	76	74	74	72
	250	85	87	93	92	90	85	79	76	73	82	83	87	81	77	75	74	73	72
	300	88	91	92	90	89	85	80	77	75	82	85	91	78	77	74	74	72	71
	350	88	90	94	91	88	85	80	77	75	87	88	91	84	81	75	71	67	66
	400	88	87	91	91	87	84	79	77	75	92	92	93	89	83	76	68	65	66
T 18 x 18	200	84	84	89	90	79	67	59	56	54	84	86	85	75	67	67	62	63	61
	250	86	89	92	86	78	70	64	62	60	84	87	86	72	68	64	63	65	63
	300	89	93	83	81	75	69	66	64	63	84	89	85	68	65	60	61	62	63
	350	90	92	90	81	75	69	67	65	62	87	90	89	77	69	61	59	59	55
	400	91	90	94	80	73	68	66	64	60	90	92	91	84	72	63	59	54	50
T 21 x 18	200	90	90	93	87	73	60	49	48	43	90	90	84	72	63	60	57	59	56
	250	90	94	88	82	72	63	55	55	50	89	91	83	68	63	58	58	63	62
	300	93	94	77	75	69	62	58	57	52	89	93	81	61	59	55	58	61	62
	350	94	96	85	76	69	62	59	57	53	89	92	87	71	64	57	57	55	53
	400	97	96	93	75	67	60	59	56	53	91	92	90	79	67	59	58	51	48

557

558 **Table 4.** *CU (%) resulting from different triangular sprinkler spacings, nozzle pressures and*
 559 *wind speeds for the RC-130H and VYR-70 sprinklers, using 4.4 and 2.4 mm nozzles.*

560

561

	P (kPa)	RC-130H										VYR-70							
		U (m s ⁻¹)										U (m s ⁻¹)							
		0	1	2	3	4	5	6	7	8	0	1	2	3	4	5	6	7	8
T 15 x 12	200	95	93	91	89	86	84	84	85	84	93	92	90	86	84	81	78	78	76
	250	95	93	91	90	88	84	85	83	80	97	95	94	90	88	84	81	81	77
	300	93	92	90	90	89	85	83	80	78	98	97	95	93	90	87	83	82	79
	350	97	95	92	90	88	87	84	80	79	99	97	95	93	89	84	80	77	78
	400	99	97	94	90	85	86	84	81	80	99	95	92	91	88	83	76	76	74
T 18 x 15	200	82	82	86	89	92	92	88	80	75	84	84	83	78	74	75	75	77	78
	250	84	85	88	91	93	89	83	78	73	88	89	87	83	81	75	72	77	76
	300	85	86	90	93	90	85	78	73	69	92	91	91	88	86	83	81	78	76
	350	88	88	90	93	89	84	77	72	70	92	92	92	89	86	80	73	68	68
	400	92	91	92	92	86	80	75	72	70	92	91	94	92	85	76	67	63	63
T 18 x 18	200	81	82	89	92	88	80	73	65	60	87	87	85	78	73	72	71	68	66
	250	83	85	91	92	84	77	70	64	61	89	90	88	82	79	72	67	70	68
	300	87	88	93	87	78	70	64	61	56	92	92	90	86	83	79	73	70	69
	350	88	88	93	89	75	67	63	61	56	93	92	91	87	79	70	65	59	56
	400	90	89	93	88	73	64	62	61	55	92	91	94	85	71	63	58	50	47
T 21 x 18	200	83	85	92	94	85	76	64	56	50	92	90	86	78	71	71	69	66	63
	250	86	88	94	90	80	72	61	57	51	92	92	87	81	77	70	64	68	68
	300	91	93	95	84	72	63	56	54	47	94	95	88	84	81	77	72	70	70
	350	90	91	95	86	70	59	56	52	49	94	94	89	84	76	67	63	59	55
	400	91	90	94	86	67	57	56	51	51	94	94	93	81	66	60	58	48	45

562

563 **Table 5.** *CU (%) resulting from different rectangular sprinkler spacings, nozzle pressures and*
 564 *wind speeds for the RC-130H and VYR-70 sprinklers, using 4.0 and 2.4 mm nozzles.*

565

566

	P (kPa)	RC-130H										VYR-70									
		U (m s ⁻¹)										U (m s ⁻¹)									
		0	1	2	3	4	5	6	7	8	0	1	2	3	4	5	6	7	8		
R 15 x 12	200	88	88	89	90	88	85	83	80	81	88	88	87	83	80	78	76	76	74		
	250	90	91	92	91	89	86	84	82	81	88	89	89	83	80	78	75	74	72		
	300	93	94	91	90	89	85	84	82	79	89	90	90	83	81	77	76	73	72		
	350	93	93	92	90	87	85	83	83	79	92	93	92	88	83	78	76	74	71		
	400	92	91	91	90	85	85	81	82	78	96	95	94	91	85	80	76	74	70		
R 18 x 15	200	88	88	88	89	84	77	73	71	68	88	87	84	77	75	73	72	72	71		
	250	90	91	91	88	85	80	76	74	72	88	88	86	78	75	73	73	72	72		
	300	93	93	86	85	83	80	78	76	74	88	89	87	77	74	74	73	72	71		
	350	93	93	89	85	83	81	77	76	74	91	91	89	82	78	75	71	68	66		
	400	93	92	92	85	81	80	76	76	73	93	93	91	87	81	77	69	65	67		
R 18 x 18	200	89	87	89	85	78	67	60	56	54	89	87	83	74	68	66	63	62	61		
	250	91	92	89	84	77	70	64	62	60	89	89	84	72	67	64	63	64	64		
	300	94	93	82	81	75	70	66	65	62	90	90	83	69	64	61	61	62	64		
	350	95	93	87	80	74	70	66	66	61	91	92	87	77	68	61	60	59	55		
	400	94	92	91	79	72	69	66	65	60	93	93	90	84	72	62	60	53	50		
R 21 x 18	200	86	85	84	79	69	58	50	47	43	86	83	77	69	62	59	58	58	56		
	250	89	88	81	77	69	62	55	54	51	87	85	78	67	62	58	59	62	62		
	300	92	87	73	72	66	61	57	56	54	87	86	75	62	57	55	58	60	63		
	350	91	89	79	73	66	61	58	57	54	91	89	81	70	63	57	56	56	54		
	400	90	89	84	71	64	60	58	56	54	95	92	86	77	67	59	56	51	48		

567

568 **Table 6.** *CU (%) resulting from different rectangular sprinkler spacings, nozzle pressures and*
 569 *wind speeds for the RC-130H and VYR-70 sprinklers, using 4.4 and 2.4 mm nozzles.*

570

571

	P (kPa)	RC-130H										VYR-70									
		U (m s ⁻¹)										U (m s ⁻¹)									
		0	1	2	3	4	5	6	7	8	0	1	2	3	4	5	6	7	8		
R 15 x 12	200	89	89	89	91	89	86	85	83	81	90	90	88	84	80	78	77	78	78		
	250	90	90	90	92	89	86	85	81	80	93	92	90	87	85	80	77	79	76		
	300	91	91	91	92	89	85	80	81	77	95	94	93	90	88	84	81	79	77		
	350	93	92	92	92	87	84	82	80	78	95	94	93	90	87	81	78	74	73		
	400	96	93	93	91	83	82	82	80	78	96	93	93	91	86	79	75	71	69		
R 18 x 15	200	87	88	89	91	89	85	81	76	73	90	89	86	80	74	74	74	75	76		
	250	88	90	90	90	88	83	79	76	72	93	92	89	83	80	74	69	77	75		
	300	91	91	91	88	84	80	76	74	68	95	94	91	87	85	81	79	77	76		
	350	92	92	92	88	83	80	76	73	70	95	93	91	87	83	79	73	70	68		
	400	93	93	93	88	80	77	75	72	70	95	93	93	87	82	76	68	63	63		
R 18 x 18	200	86	87	91	89	86	79	72	65	61	91	89	85	79	72	72	70	68	67		
	250	88	89	92	88	83	77	70	64	61	93	93	88	83	78	72	67	71	69		
	300	92	91	92	85	77	70	64	63	56	96	95	91	86	83	79	74	71	71		
	350	92	92	94	87	75	67	63	62	56	96	94	91	86	79	71	64	61	57		
	400	93	92	95	87	73	64	63	61	56	96	94	93	84	71	64	59	50	47		
R 21 x 18	200	87	88	86	84	78	72	63	56	50	88	86	81	74	68	68	66	65	62		
	250	89	89	87	82	75	69	61	56	51	91	89	83	78	74	69	63	68	68		
	300	89	89	85	77	68	62	55	54	48	93	91	85	80	78	74	72	70	70		
	350	92	92	88	79	67	59	55	53	49	94	91	85	80	75	67	63	60	55		
	400	95	94	90	80	65	56	55	52	50	94	90	85	76	64	61	57	48	45		

572

577 **List of Figures**

578 **Figure 1.** *Differences in the coefficient of uniformity (CU, %) measured using Small (S),*
579 *Medium (M) and Large (L) catch cans as a function of wind speed (U , $m s^{-1}$).*

580 **Figure 2.** *a) Experimental vs. calibration coefficients of uniformity (CU_e and CU_c ,*
581 *respectively) for the RC-130H and VYR-70 sprinklers; and b) Experimental vs. validation*
582 *coefficients of uniformity (CU_e and CU_v , respectively). The dashed line represents the 1:1*
583 *relationship.*

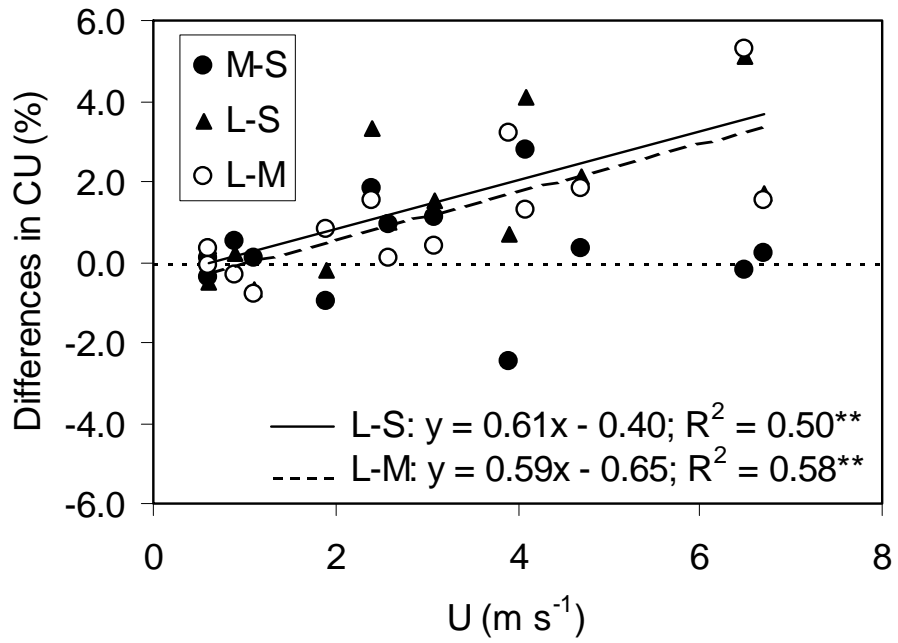
584 **Figure 3.** *Additional validation experiments performed using both sprinklers and different*
585 *operating pressures and spacings. The nozzle diameters were 4.4 ± 2.4 mm in all cases. The*
586 *subfigures present experimental and simulated values of CU as a function of wind speed (U ,*
587 *$m s^{-1}$).*

588

589 **Figure 1.** Differences in the coefficient of uniformity (CU, %) measured using Small (S),
590 Medium (M) and Large (L) catch cans as a function of wind speed (U , $m s^{-1}$).

591

592

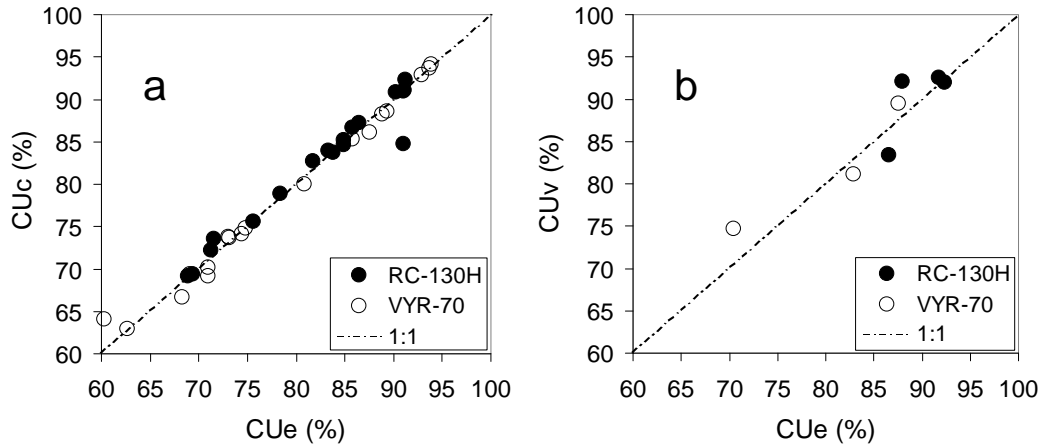


593

594

595 **Figure 2.** a) Experimental vs. calibration coefficients of uniformity (CUe and CUc,
 596 respectively) for the RC-130H and VYR-70 sprinklers; and b) Experimental vs. validation
 597 coefficients of uniformity (CUe and CUv, respectively). The dashed line represents the 1:1
 598 relationship.

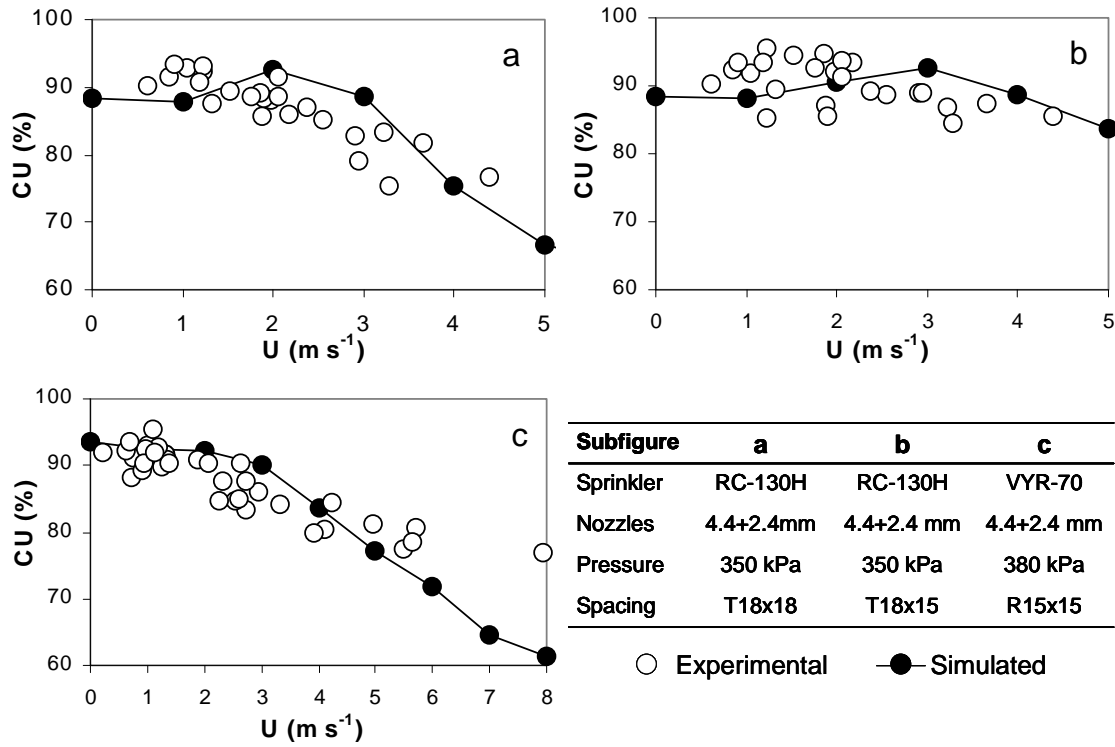
599



600

601 **Figure 3.** Additional validation experiments performed using both sprinklers and different
 602 operating pressures and spacings. The nozzle diameters were 4.4 + 2.4 mm in all cases. The
 603 subfigures present experimental and simulated values of CU as a function of wind speed (U ,
 604 $m s^{-1}$).

605



606